BULLETIN OF THE POLISH ACADEMY OF SCIENCES
TECHNICAL SCIENCES, Vol. 71(2), 2023, Article number: e144607
DOI: 10.24425/bpasts.2023.144607

Influence of ageing on microstructure and mechanical properties of TP347HFG austenitic stainless steel

Grzegorz GOLAŃSKI[1]* **and Hanna PURZYŃSKA**[2]

[1] Czestochowa University of Technology, Department of Materials Engineering, Armii Krajowej 19, 42-200 Częstochowa, Poland
[2] Łukasiewicz Research Network – Upper Silesian Institute of Technology, K. Miarki 12-14, 44-100 Gliwice, Poland

Abstract. The paper presents the results of microstructural and mechanical investigation of long-term aged TP347HFG austenitic stainless steel. Ageing was performed at a time of up to 30 000 hours and the temperature of 600 and 650°C. Ageing was proved to lead to the precipitation of secondary phase particles not only inside grains but also on the boundaries of grains and twins. The MX precipitates were observed inside the grains. However, $M_{23}C_6$ carbides and sigma phase precipitates were observed on grain boundaries. The changes in the microstructure of the examined steel translated into the mechanical properties, i.e. initially observed growth and then the decrease of yield strength and a gradual decrease in impact energy. The overageing process – a decrease in strength properties – was associated with the growth of the size of $M_{23}C_6$ carbides and the precipitation of the sigma phase. The reduction of impact energy in TP347HFG austenitic stainless steel was found to be associated with the precipitation of $M_{23}C_6$ carbides in the case of the 600°C temperature, and the $M_{23}C_6$ carbides and sigma phase in the case of the 650°C temperature. The rate of changes in the microstructure and mechanical properties depended on the ageing temperature.

Key words: austenitic stainless steel; precipitates; microstructure; mechanical properties.

1. INTRODUCTION

The efforts to reduce the harmful impact of industry on the environment resulted in implementing the process of decarbonising the economy, among others. In the case of thermal energy, the emission of pollutants into the atmosphere is reduced by increasing electricity production with the use of renewable energy sources (RES). However, due to periodic efficiency (wind and solar activity), RESs are very unstable in terms of production and require stabilising protection in the form of conventional coal power units [1,2]. On the other hand, reducing the negative impact of burning fossil fuels in power units on the natural environment is associated with increasing their efficiency as a result of increasing steam parameters. The increase in efficiency was possible as a result of applying modern heat-resistant alloys with a ferritic and austenitic matrix to the key, critical components of the power unit installation [3, 4].

Austenitic alloys were introduced in the power industry as construction materials because of the low microstructure stability of martensitic steels of the 12%Cr type (HCM12A, VM12), and in the case of the steel of the 9%Cr type, because of their insufficient resistance to oxidation and high-temperature corrosion [5, 6]. One of the representatives of the group of creep-resisting steels with an austenitic matrix that has found application in the critical components of coal-fired units working at supercritical parameters was TP347HFG steel [7]. TP347HFG steel belongs to a group of heat-resistant austenitic steels used in the power industry for steam superheaters, among other things. This type of steel was designed on the basis of TP347H steel by obtaining a fine-grained structure through applying properly selected parameters of thermoplastic treatment. Because of fine grain, TP347HFG steel shows better resistance to corrosion and oxidation compared to the base steel with similar creep resistance [7].

Previous studies on creep-resistant austenitic steels were mostly concentrated on the HR3C and Super 304H steel grades or focused on the investigation of material after use. These studies proved that the dominant mechanism of both the strengthening and degradation of the microstructure of austenitic steel involves the processes connected with precipitation and the coagulation of secondary phases [4, 8–10]. However, there is a lack of comprehensive data concerning the influence of the effect of temperature and time of ageing, simulating the actual use, on the processes of degradation of microstructure and mechanical properties of TP347HFG steel. The paper presents the influence of temperature and time of ageing on the change of microstructure and mechanical properties of TP347HFG steel after long-term ageing for up to 30 000 hours at 600 and 650°C.

2. SPECIMENS

The testing material consisted of samples from tube sections made of TP347HFG steel with the following dimensions: 50.8 × 11.5 mm (outer diameter x wall thickness). The chemical composition of the tested steel is presented in Table 1. The tested steels were subjected to ageing at 600 and 650°C and ageing for up to 30 000 hours.

*e-mail: grzegorz.golanski@pcz.pl

Manuscript submitted 2022-09-14, revised 2022-11-10, initially accepted for publication 2022-12-08, published in April 2023.

Table 1
Chemical composition of steel, wt%

C	Si	Mn	P	S	Cr	Ni	Nb	N
0.10	0.38	1.42	0.022	0.001	18.71	11.88	0.60	0.10

3. METHODOLOGY

The scope of the conducted studies included: chemical composition analysis, microstructure studies using scanning electron microscope (SEM) and transmission electron microscope (TEM), analysis of precipitates using electron diffraction, computer image analysis, testing of mechanical properties: static tensile test and impact test. The chemical composition analysis was performed using a SpectroLab spark spectrometer. The microstructural investigation was carried out using Jeol JSM-6610LV – SEM and TITAN 80–300 – TEM. The specimens for SEM tests were prepared by grinding with papers of different grits, polishing and subsequent etching in the Mi19Fe reagent. The specimens for TEM tests, i.e. thin films, were prepared as a disc of 3 mm in diameter and approx. 100 µm in thickness electrolytically thinned to perforation using a solution of 20% perchloric acid in ethanol at a temperature of approx. –30°C and voltage of approx. 20 V. The microsection surfaces were oriented perpendicularly to the axis of the pipe section. The identification of the precipitates on thin films was performed using selective electron diffraction. The static tensile test was carried out on round samples with an initial measuring diameter of up to 5 mm using a Zwick/Roell Z100 testing machine with a force range of up to 100 kN. The impact test was carried out on standard Charpy V samples.

4. MICROSTRUCTURE IN THE DELIVERY CONDITION

An example of the microstructure of the tested steel in the delivered condition is shown in Fig. 1a. As delivered, the investigated alloy was characterized by austenitic microstructure with numerous twins and precipitates arranged both in a random and banded manner. The tested material in the as-received state was characterized by a grain size number equal to 9. The TP347HFG steel belongs to the group of heat-resistant austenitic steels stabilized with strongly carbide-forming alloying element-niobium (Table 1). This results in the presence of large primary niobium-rich precipitates in the microstructure at delivery (Fig. 1b). These particles are precipitated in the last stage of solidification [4, 9, 11], therefore some of them are observed near or at grain boundaries (Fig. 1a, 1b). The content of Nb in the chemical composition of austenitic steels is at such a level as to allow only partial binding of carbon and nitrogen atoms. This allows for the precipitation of Cr-rich precipitates in the grain boundaries, reducing the creep rate due to slippage inhibition at the boundaries [4, 9]. In addition to the large primary niobium-rich particles, the microstructure of this steel also reveals numerous dispersed precipitates inside the grains (Fig. 2).

Thermomechanical heat treatment of this type of steel, as a result of modification of temperature-time parameters, facilitated the separation of dispersed particles, which resulted in obtaining a fine-grained structure with a grain size of at least 7 [7]. The performed identifications showed that both large, primary and dispersed particles inside the grains are MX precipitates. The presence of numerous, both coherent and non-coherent with the matrix of twins, in the microstructure of the tested steel, proves the low stacking fault energy of the steel [7, 10].

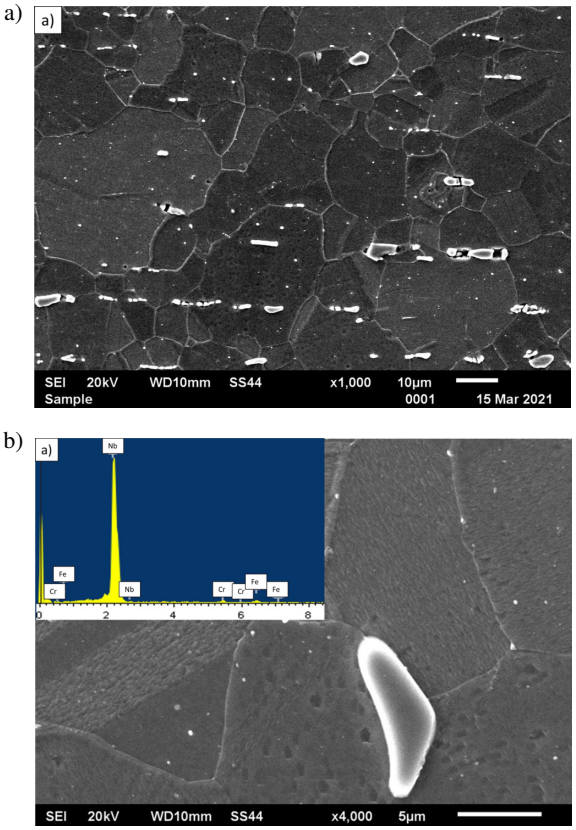

Fig. 1. The microstructure of TP347HFG steel in delivery condition (a); niobium-rich primary precipitate at grain boundary (b); SEM

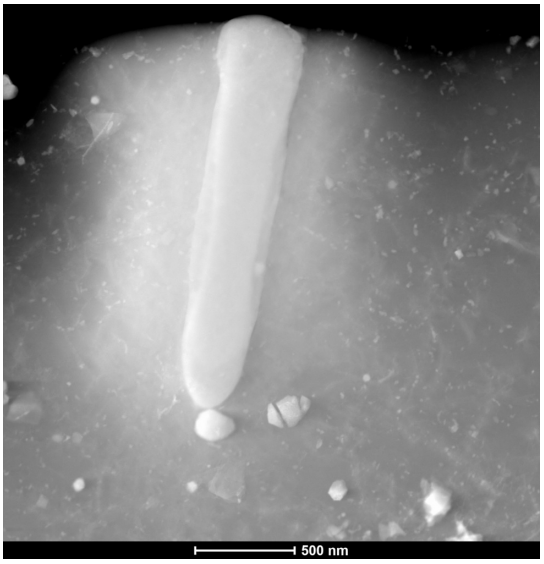

Fig. 2. Large and dispersed MX precipitates in the steel, TEM

The presence of numerous twins in the austenitic matrix not only translates into the growth of plasticity and ductility, and the limitation on susceptibility to brittle cracking, but it also raises the resistance of austenitic steel to intercrystalline corrosion [8, 9]. Apart from MX precipitates in the as-received state inside the grains, as well as on grain boundaries and twin boundaries, no other types of precipitates were noticed.

5. MICROSTRUCTURE AFTER AGEING

Austenitic steels in a solution heat-treated state are characterized by a metastable structure, which in the case of increased/high temperature will result in gradual changes in the microstructure of these materials. In austenitic steels, the basic process of degradation of their microstructure is precipitation processes occurring both at grain boundaries, twin boundaries, as well as inside the grains [4, 10, 12]. The dynamics of changes in the microstructure of austenitic steels depend on temperature as a factor that has a decisive influence on diffusion processes.

In the initial period of ageing, both at 600°C and 650°C, precipitation processes occurring mainly at grain boundaries were observed (Fig. 3). Boundaries, as surface defects, are places of privileged precipitation of secondary phase particles and segregation of impurities thereto. This is due to the fact that these areas are characterized by higher interfacial energy and faster diffusion rate compared to the grain interior. In austenitic steels, $M_{23}C_6$ carbides precipitate on grain boundaries (Fig. 4). The precipitation of $M_{23}C_6$ carbides along grain boundaries is related to the limited solubility of carbon in austenite [9]. The $M_{23}C_6$ carbides precipitate successively on grain boundaries, incoherent and coherent twin grain boundaries, and finally intragranular boundaries. Longer ageing times contributed to an increase in the number and local formation of a continuous network of precipitates and then the coagulation of these particles (Figs. 3, 5a, 5c). The changes in the morphology of $M_{23}C_6$ carbides resulted mainly from the low stability of these particles. In the tested steel, after longer ageing times at 650°C, mainly at the contact of the three-grain boundaries, a morphologically different precipitate was revealed – intermetallic sigma phase (Figs. 5b, 5d, 6). The precipitation of the sigma phase, the growth of its size and volume fraction is a very sluggish process, which is connected, among other things, with the very slow diffusion of a substitutional element in austenite. The sigma phase is incoherent with austenite and its nucleation is difficult [9, 12–14]. The sigma phase in austenitic steel can precipitate in three ways, including the transformation from austenite – to – sigma phase, the transformation from δ ferrite – to – sigma phase and *in situ* transformation of $M_{23}C_6$ carbides [12, 13]. Since the sigma phase is a precipitate rich in iron and chromium, according to [14], the preferential place of its precipitation and further growth is the inter-phase boundary $M_{23}C_6$ carbide/matrix. The metastable chromium-rich $M_{23}C_6$ carbide can easily provide the required chromium atoms for the nucleation of sigma phases during its dissolution.

Additionally, as shown in [15], the sigma phase may precipitate due to the *in-situ* transformation of $M_{23}C_6$ carbides at grain boundaries, which is accompanied by the dissolution of these

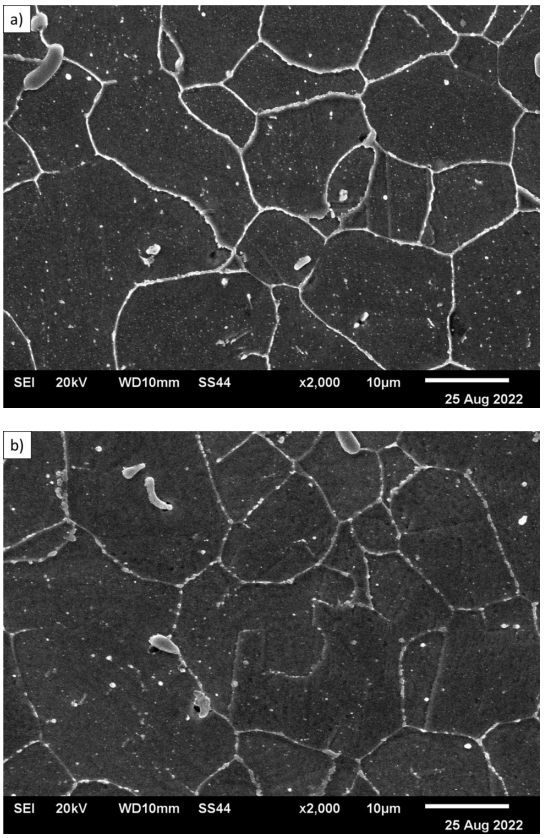

Fig. 3. Microstructure of TP347HFG steel after and 1000 hours of ageing at a) 600°C; b) 650°C, SEM

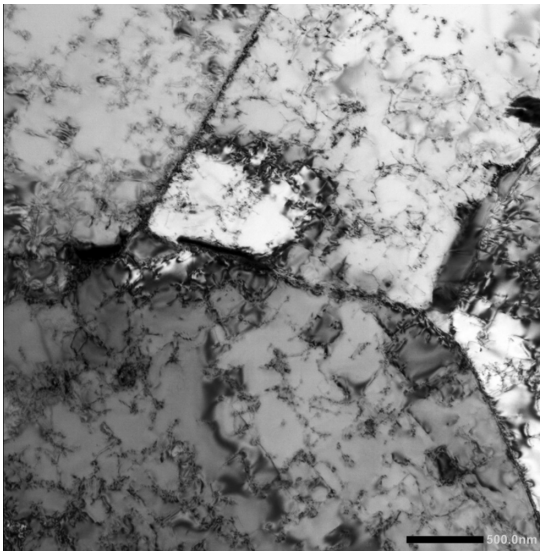

Fig. 4. The precipitates on the grain/twin boundaries and inside grains, TEM

carbides. The microanalysis of the chemical composition of the sigma phase also proved the presence of silicon in this phase (Fig. 6b). Silicon has a significant effect not only on the rate of precipitation of this phase but also on its volume fraction [16].

In steel aged at a temperature of 650°C, a relative increase in the size and surface proportion of the sigma phase precipitates with ageing time (Figs. 5b, 5d) was visible, which results from

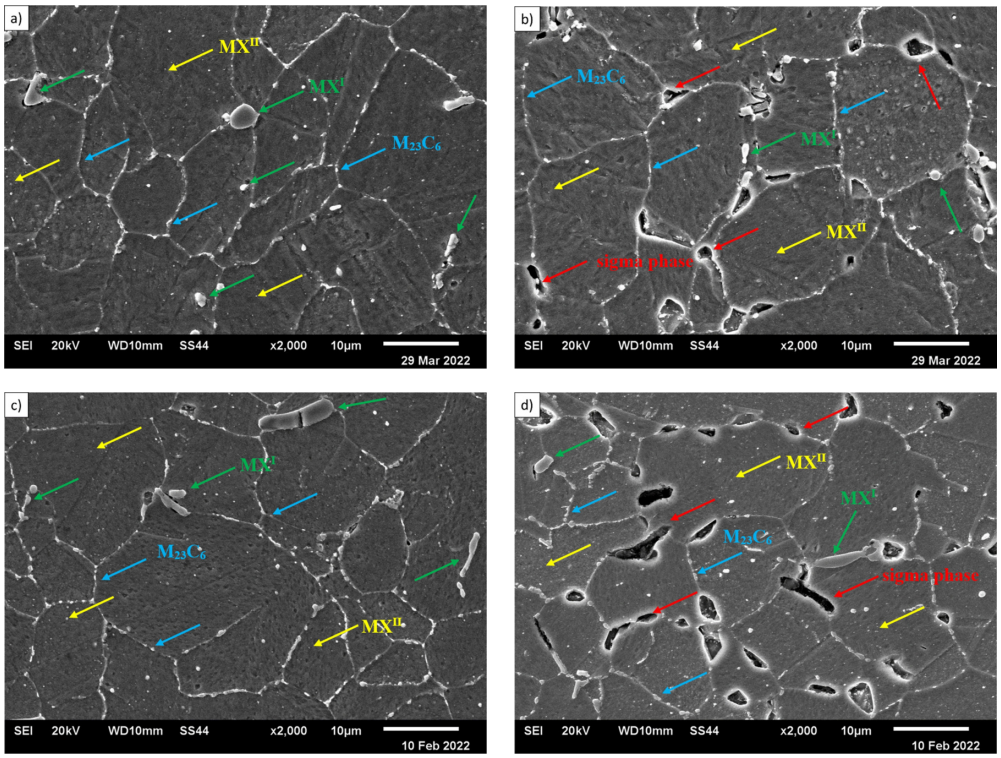

Fig. 5. Microstructure of TP347HFG steel after 20 000 (a, c) and 30 000 (b, d) hours of ageing at a, b) 600°C; c, d) 650°C, where: MX^I – primary particles; MX^{II} – fine particles, SEM

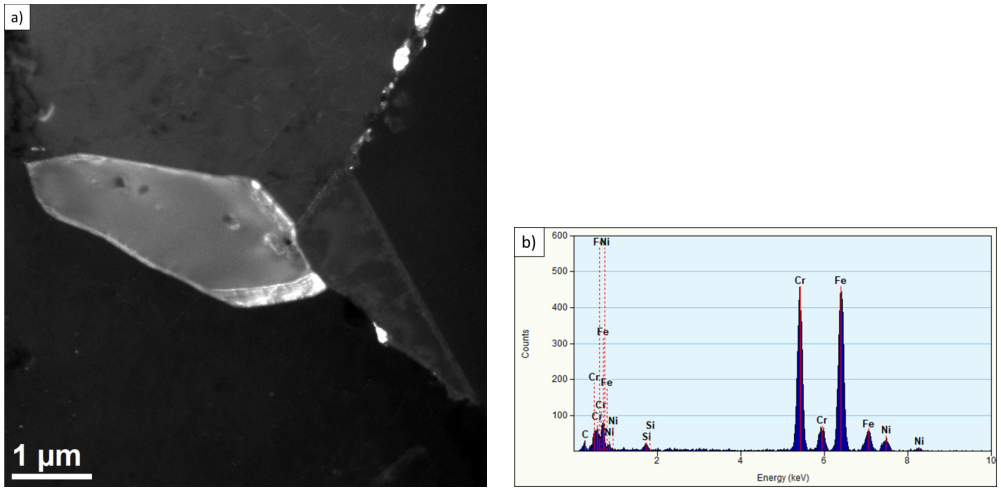

Fig. 6. Sigma phase precipitate in TP347HFG steel aged for 30 000 hours at 650°C; a) dark field; b) X-ray spectrum, TEM

the high tendency of the sigma phase to coagulate. The growth of the sigma phase probably took place at the expense of the atrophy of some of the metastable $M_{23}C_6$ carbides separated at boundaries, which are the reservoir of Cr atoms. The lack of solubility in the sigma phase of carbon atoms, perhaps, according to [14], as a result of their diffusion at grain boundaries, contributes to the increase in the size of $M_{23}C_6$ carbides precipitated at the boundaries. On the other hand, according to [9, 12], C atoms enrich border regions, which translates into the potential possibility of the precipitation of $M_{23}C_6$ carbides inside the grains and at the ends of twin boundaries.

At a lower ageing temperature of 600°C, no sigma phase precipitates were observed in the microstructure of the tested steel, even after the time of 30 000 hours of holding. This indicates that the process of nucleation and growth of sigma precipitates depends not only on the chromium content but also on the ageing temperature.

Inside the grains, similarly as in the as-received state, apart from large precipitates, the presence of dispersed NbX precipitates was observed (Figs. 2, 7). The dispersed nanometric NbX particles, relatively evenly distributed in the matrix, constitute an effective obstacle for the movement of dislocations (Fig. 7).

They anchor and inhibit the possibility of dislocation movement, and thus contribute to a considerable strengthening of the examined steel with the precipitation mechanism [3,12,17]. The high susceptibility of C and N atoms to segregate to the dislocation line [12, 17] is why a part of those precipitates was seen on the dislocations, which caused their accumulation. These precipitates are also characterized by a significant property in terms of long-term use of steel, i.e. the low susceptibility to coagulation [11, 18].

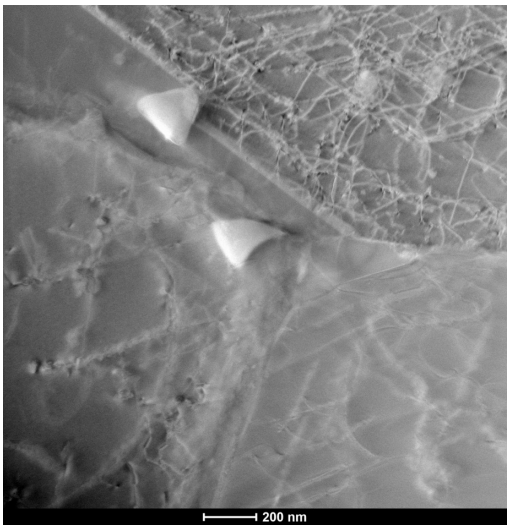

Fig. 7. Effect of dislocation with dispersed MX precipitates inside the grains, TEM

6. EFFECT OF AGEING ON THE MECHANICAL PROPERTIES OF TP347HFG STEEL

The degradation of the microstructure of the examined steel translates into changes in its original mechanical properties. In the as-received state, due to the dominant solution-based mechanism of strengthening and a large number of slip bands, the analyzed alloy, similar to other austenitic steels, is characterized by high ductility and plasticity, with relatively low strength properties (Figs. 8, 9). As a result of the occurring precipitation processes, the ageing of the tested steel contributed to an increase in strength properties – yield strength (YS) and tensile strength (TS) – Fig. 8. The initial increase of the value of YS was observed regardless of the ageing temperature until the annealing time of 5000 hours. Longer ageing times contributed to the decrease in the value of this parameter (Fig. 8a). In the case of TS (Fig. 8b), a continuous increase of this parameter was observed until the ageing time of 30 000 hours. Higher increases in both YS and TS were observed for the alloy aged at a lower temperature. The increase in strength properties is related to the limitation of the free movement of dislocations.

In austenitic steels, the precipitation of secondary dispersed particles is the dominant strengthening mechanism contributing to the increase in these properties. The influence of this strengthening is mainly related to the type and morphology of the precipitates. Dispersive, nanometric particles and precipitates with a plate shape, in comparison with a round shape, at equal volume fractions ensure a higher strengthening gain [19]. According to calculations [20], the stress needed to bypass a particle – secondary NbC precipitate – with the Orowan mechanism amounts to 27 MPa, whereas according to [16], this value amounts to 58 MPa. However, the stress for $M_{23}C_6$ carbide in austenitic steel was estimated to be 10 MPa [20]. Moreover, in [21], the authors point to a negligibly small role of $M_{23}C_6$ carbides in the strengthening of austenitic steel. The calculations made for Super 304H steel showed that the pinning force of $M_{23}C_6$ carbides, compared to dispersed precipitates of the Z phase and ε_Cu particles, is respectively 10 and 27 times smaller [22]. In turn, according to [9], $M_{23}C_6$ carbides play an important role in shaping high-temperature strength. This indicates a significant role of MX dispersed precipitates as the phase that dominates the precipitation hardening of the tested steel.

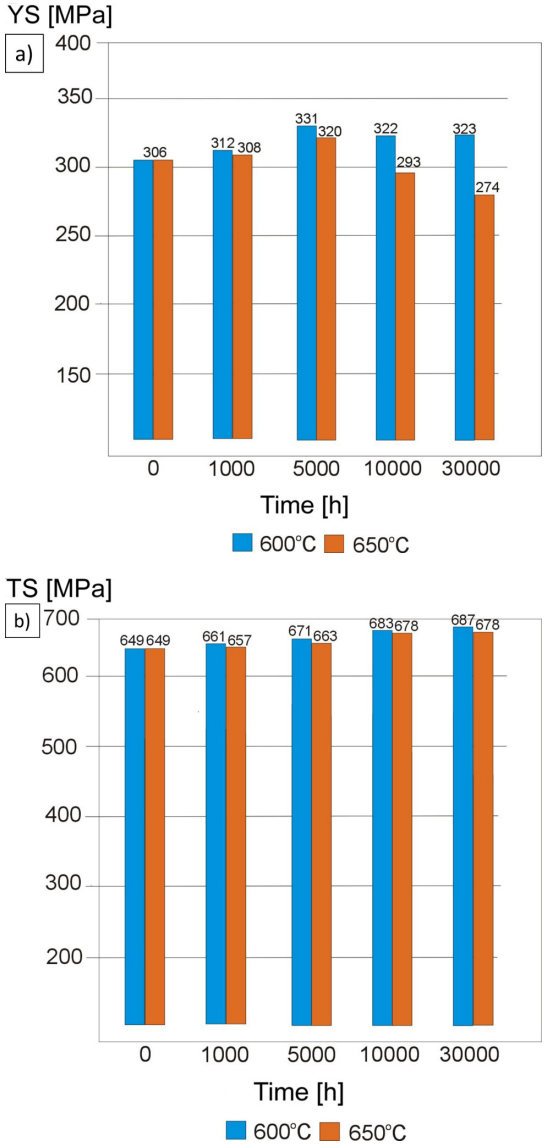

Fig. 8. Change in the value of yield strength (a) and tensile strength (b) of TP 347HFG steel depending on ageing parameters

The visible effect of overageing (Fig. 8a), in general, is related to the process of precipitate coagulation and the disappearance of the coherence of strengthening particles of secondary phase particles. The overageing effect in the tested steel should be associated mainly with the coagulation of $M_{23}C_6$ carbides and the precipitation and increase in the size of the sigma phase particles at the expense of dissolving $M_{23}C_6$ carbides. The higher thermal stability of MX precipitates (–70 kJ/mol [23]) compared to $M_{23}C_6$ carbides (–20 kJ/mol [23]), or the sigma phases and the coherent or semi-coherent boundary of MX particles translates into their very slow coagulation rate. The above results in a more effective interaction of MX precipitates acting as barriers to dislocation traffic compared to other precipitates. Nevertheless, as demonstrated in [20–22], even a slight increase in the size of the dispersed particles causes quite a significant reduction in the pinning force. Moreover, the precipitation and coagulation of the secondary phase particles lead to the depletion of the matrix in the alloying elements diffusing into these precipitates. This results in a reduction of the strengthening by the solution mechanism, which translates into a decrease in YS.

Changes in the microstructure of the tested steel during ageing also reduce its impact energy (KV) – Fig. 9. The change in the KV value, regardless of the ageing temperature, was comparable to the holding time of 5000 hours (Fig. 9). Longer ageing times at 650°C result in an accelerated reduction of this parameter as compared to the change in KV after ageing at 600°C (Fig. 9). The toughness of the steel depends mainly on the grain size, the distribution of the precipitates in the matrix and their volume fraction precipitated at grain boundaries. The fine-grained structure of the tested steel (grain size of at least 7 according to the standard scale) and the presence of numerous twins in the microstructure (Fig. 1) significantly reduce the tendency of the analyzed alloy to brittle fracture. The boundaries of grains and twins constitute an energy barrier for low-energy propagation of cracking. Additionally, [24] showed that the positive effect of fine grain is connected with the discontinuous distribution of carbides at grain boundaries. The beneficial effect of the fragmentation of the heat-resistant steel structure on toughness and the brittle state transition temperature was also demonstrated in [8, 15].

In turn, the coarse-grained structure of HR3C steel (grain size at most 3–4 according to the standard scale) was indicated as a significant cause of the brittleness of this steel during use [9]. The decrease in KV of the tested steel was related to the precipitation processes taking place both at grain boundaries and at the boundaries of twins (Figs. 3–6). In steel aged at 600°C and in the initial stage of ageing at 650°C (up to 5000 hours), the reduction of KV resulted from the precipitation of $M_{23}C_6$ carbides at grain boundaries. The appearance of sigma phase particles in the microstructure of steel aged at 650°C (Figs. 5b, 5d, 6) translated into an accelerated reduction of KV.

The decisive influence of the sigma phase precipitation on the brittleness of the welded joint of Super 304H steel was also demonstrated in [25]. The $M_{23}C_6$ carbides precipitated along grain boundaries and twin boundaries as well as hard and brittle sigma phase particles precipitated along grain boundaries in steel aged at a higher temperature contributed to the reduction

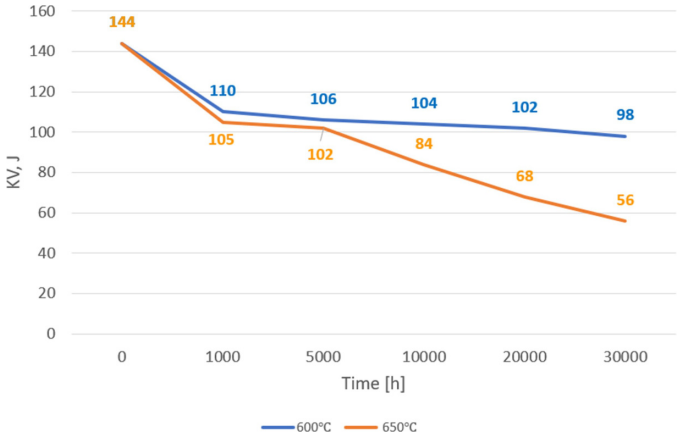

Fig. 9. Influence of ageing parameters on the change of impact energy of TP347HFG steel

of the strong cohesion of grain boundaries, which in turn contributed to the low-energy, brittle fracture propagation.

Moreover, the presence of sigma phase precipitates on the boundaries of grains facilitates and favours faster nucleation of microcracks and cavities [9]. According to [13], the crack resistance of austenitic steels is also strongly affected by the morphology of the precipitates of $M_{23}C_6$ carbides and sigma phase, precipitated on the boundaries. The reduction of toughness and YS is also influenced by the decrease in the density of twins in the microstructure that occurs during ageing [9, 15, 22].

7. CONCLUSIONS

The conducted tests of long-term aged TP347HFG steel at 600 and 650°C facilitated the formulation of the following conclusions:

1. Ageing of TP347HFG steel leads to changes in its microstructure, mostly appearing through the precipitation processes. $M_{23}C_6$ carbides are precipitated on the boundaries of grains, whereas after longer times of ageing at 650°C also the sigma phase precipitates are observed. Inside the grains, the presence of primary and dispersive MX particles was observed.
2. Changes in precipitate morphology initially contributed to an increase in the strength properties – yield strength (YS), from the value of 306 MPa in the as-received condition to the level of 331 and 320 MPa for the temperature of 600 and 650°C, respectively. The longer aging times resulted in an aging effect, which resulted in a gradual reduction of YS, to a value of 274 MPa for a temperature of 650°C, that is, a value lower than in the as-received condition.
3. The nucleation and growth of $M_{23}C_6$ carbides at the grain/twin boundaries contribute to the gradual reduction of the impact energy from the level of 144 J in the as-received state to the value of 98 J after 30 000 hours of aging at 600°C. The precipitation of the sigma phase in steel aged at 650°C accelerates the embrittlement of the tested steel, the impact energy after 30 000 hours of aging in this case was 56 J.

REFERENCES

[1] J. Jurasz and J. Mikulik, "Economic and environmental analysis of a hybrid solar, wind and pumped storage hydroelectric energy source: a Polish perspective," *Bull. Pol. Acad. Sci. Tech. Sci.*, vol. 66, no. 6, pp. 859–869, 2017, doi: 10.1515/bpasts-2017-0093.

[2] M. Bartecka, P. Terlikowski, M. Kłos, and Ł. Michalski, "Sizing of prosumer hybrid renewalble energy systems in Poland," *Bull. Pol. Acad. Sci. Tech. Sci.*, vol. 68, no. 4, pp. 721–731, 2020, doi: 10.24425/bpasts.2020.133125.

[3] A. Iseda, H. Okada, H. Semba, and M. Igarashi, "Long term creep properties and microstructure of SUPER304H, TP347HFG and HR3C for A-USC boilers," *Energy Mater.*, vol. 2 no. 4, pp. 199–206, 2007, doi: 10.1179/174892408X382860.

[4] A. Zieliński, R. Wersta, and M. Sroka, "Analysis of the precipitation process of secondary phases after long-term ageing of S304H steel, "*Bull. Pol. Acad. Sci. Tech. Sci.*, vol. 69, no. 5, pp. 1–7, 2023, doi: 10.24425/bpasts.2023.137520.

[5] R.O. Kaibyshev, V.N. Skorobogatykh, and I.A. Shchen-kova, "Formation of the Z-phase and prospects of martensitic steels with 11%Cr for operation above 590°C," *Metal Science and Heat Treatment*, vol. 52, pp. 90–99, 2010, doi: 10.1007/s11041-010-9239-0.

[6] T. Dudziak, T. Hussain, and N.J. Simms, "High-temperature performance of ferritic steels in fireside corrosion regimes: temperature and deposits," *J. Mater. Eng. Perform.,* vol. 26, pp. 84–93, 2017, doi: 10.1007/s11665-016-2423-7.

[7] K. Yoshikawa, H. Teranishi, K. Tokimasa, H. Fujikawa, M. Miura, and K. Kubota, "Fabrication and properties of corrosion resistant TP347H stainless steel," *Journal of Materials Engineering*, vol. 10, pp. 69–84, 1988, doi: 10.1007/BF02834116.

[8] A. Zieliński, R. Wersta, and M. Sroka, "The study of the evolution of microstructure and creep properties of Super 304H austenitic stainless steel after aging for up to 50 000 h," *Arch. Civ. Mech. Eng.,* vol. 22, no. 2, pp. 1–24, 2022, doi: 10.1007/s43452-022-00408-6.

[9] A. Zieliński, G. Golański, and M. Sroka, "Evolution of the microstructure and mechanical properties of HR3C austenitic stainless steel after ageing for up to 30,000 h at 650–750°C," *Mater. Sc. Eng.*, vol. 796A, p. 139944, 2020, doi: 10.1016/j.msea.2020.139944.

[10] K. Ogawa, Y. Sawaragi, N. Otsuka, H. Hirata, A. Natori, and S. Matsumoto, "Mechanical and corrosion properties of high strength 18%Cr austenitic stainless steel weldment for boiler," *ISIJ Int.*, vol. 35, no. 10, pp. 1258–1264, 1995, doi: 10.2355/isijinternational.35.1258.

[11] X.F. Zhang, H. Terasaki, and Y. Komizo, "In situ investigation of structure and stability of niobum carbonotrides in an austenitic heat-resistant steel," *Sc. Mater*., vol. 67, pp. 201–204, 2012, doi: 10.1016/j.scriptamat.2012.04.019.

[12] G. Golański, A. Zieliński, and H. Purzyńska, "Precipitation process in creep-resistant austenitic steels," in *Austenitic Stainless Steels*, Borek W., Tański T., Brytan Z., Eds. InTech Publ., 2017; pp. 93–112, doi: 10.5772/intechopen.70941.

[13] D.M.E. Villanueva, F.C.P. Junior, R.L. Plaut, and A.F. Padilha, "Comparative study on sigma phase precipitation of three types of stainless steels: austenitic, superferritic and duplex," *Mater. Sc. Techn*., vol. 22, no. 9, pp. 1098–1104, 2006, doi: 10.1179/174328406X109230.

[14] Q.-Q. Ren, Y. Yamamoto, M.P. Brady, and J.D. Poplaw-sky, "Sigma phase evolution and nucleation mechanisms revealed by atom probe tomography in a 347 stainless steel," *Materialia*, vol. 24, p. 101485, 2022, doi: 10.1016/j.mtla.2022.101485.

[15] K. Guan, X. Xu, and Z. Wang, "Effect of aging at 700°C on precipitation and toughness AISI 321 and AISI 347 austenitic stainless steel welds," *Nucl. Eng. Des.*, vol. 235, pp. 2485–2494, 2005, doi: 10.1016/j.nucengdes.2005.06.006.

[16] D.-Y. Lin, T.-Ch. Chang, and G.L. Liu, "Effect of Si content on the growth behavior of σ phase in SUS 309L stainless steels," *Sc. Mater.,* vol. 39, no. 9, pp. 855–860, 2003, doi: 10.1016/S1359-6462(03)00481-0.

[17] Ch. Solenthaler, M. Ramesh, P.J. Uggowitzer, and R. Spolenak, "Precipitation strengthening of Nb-stabilized TP347 austenitic steels by a dispersion of secondary Nb(C, N) formed upon a short-term hardening heat treatment," *Mater. Sc. Eng*., vol. 647A, pp. 294–302,2015, doi: 10.1016/j.msea.2015.09.028.

[18] J. Erneman, M. Schwind, H.-O. Adren, J.-O. Nilsson, A. Wilson, and J. Agren, "The evolution of primary and secondary niobum carbonotrides in AISI 347 stainless steel during manufacturing and long-term ageing," *Acta Mater.,* vol. 45, no. 1, pp. 67–76, 2006, doi: 10.1016/j.actamat.2005.08.028.

[19] M.R. Ahmadi, E. Povoden-Karadeniz, B. Sonderegger, K.I. Öksüz, A. Falahati, and E. Kozeschnik, "A model for coherency strengthening of large precipitates," *Scr. Mater.,* vol. 84-85, pp. 47–50, 2014, doi: 10.1016/j.scriptamat.2014.04.019.

[20] L. Li and X. Wang, "Strengthening mechanism and creep rupture behavior of advanced heat–resistant steel SA-213 S31035 for A-USC power plants," *Mat. Sci. Eng.,* vol. 775A, 138991, 2020, doi: 10.1016/j.msea.2020.138991.

[21] R. Zhou and L. Zhu, "Growth behavior and strengthening mechanism of Cu – rich particles in Sanicro 25 austenitic heat–resistant steel after aging at 973 K," *Mater. Sci. Eng. A,* vol. 796, p. 139973, 2020, doi: 10.1016/j.msea.2020.139973.

[22] L. Zhang, L. Zhu, and Z. Lu, "Microstructural evolution and the effect on mechanical properties of S30432 heat–resistant steel during aging at 650°C," *ISIJ Inter.,* vol. 50, pp. 596–600, 2010, doi: 10.2355/isijinternational.50.596.

[23] F.B. Pickering, "Historical development and microstructure of high chromium ferritic steels for high temperature applications," in *Microstructural development and stability in high chromium ferritic power plant steels*, A. Strang and D.J. Gooch, Eds. The Institute of Materials Cambridge, London, 1997, pp. 1–29.

[24] H. Wang, Y. Li, D. Chen, and J. Sun, "Precipitate evolution the ageing of Super304H steel and its influence on impact toughness," *Mater. Sc. Eng.*, vol. 754A, pp. 238–245, 2019, doi: 10.1016/j.msea.2019.03.086.

[25] J. Horvath, P. Kral, and J. Janovec, "The effect of σ-phase formation on long-term durability of welding joints in Super 304H," *Acta Phys. Pol. A*, vol. 130, no. 4, pp. 960–962, doi: 10.12693/APhysPolA.130.960.